THE ASTROPHYSICAL JOURNAL, 383:250–262, 1991 December 10

SPHERICAL ACCRETION ONTO BLACK HOLES: A COMPLETE ANALYSIS OF STATIONARY SOLUTIONS

LUCIANO NOBILI, ROBERTO TUROLLA, AND LUCA ZAMPIERI
Department of Physics, University of Padova, Via Marzolo 8, 35131 Padova, Italy
Received 1991 February 8; accepted 1991 June 18

ABSTRACT

The problem of stationary, spherical accretion onto a Schwarzschild hole is here reinvestigated by the construction of a self-consistent model which incorporates all relevant physical processes taking place in an astrophysical plasma, apart from the presence of magnetic fields and dissipative processes. In particular, transfer of radiation through the accreting gas is treated in full generality using a completely relativistic formalism. A careful analysis of critical points and boundary conditions for radiation hydrodynamics equations is performed. The complete topology of solutions in the accretion rate–luminosity plane is obtained, showing the existence of two distinct branches of models with very different emission properties: stationary accretion reveals, therefore, a bimodal behavior. By means of a self-consistent study of the effects of Compton heating, both the upper and the lower bounds for the existence of high-luminosity solutions were derived. The stability of the two possible accretion regimes is also briefly discussed.

Subject headings: accretion — black holes — hydrodynamics — radiative transfer — relativity

1. INTRODUCTION

In the last 20 years many aspects of stationary, spherical accretion onto black holes have been investigated in great detail. Starting from the pioneering work by Bondi (1952), who first pointed out the existence of a critical point in accretion flows, a great deal of work was devoted to understanding the properties of accretion, allowing for more and more complex input physics in the attempt to construct a satisfactory, self-consistent description of this phenomenon. The final goal of these studies was primarily to obtain the net energy output emitted as electromagnetic radiation by the infalling gas in connection with applications of black hole accretion to several classes of astrophysical sources. In this respect preliminary investigations on the hydrodynamics of spherical accretion proved to be of key importance in shedding light on fundamental issues like the role played by the sonic point in determining the uniqueness of the solution. The relativistic generalization of the Bondi problem considered by Michel (1972) and Begelman (1978) (see also Novikov & Thorne 1973) demonstrated, in fact, that spherical accretion onto a Schwarzschild hole must be necessarily transonic and that, once the state of the gas far from the hole is specified, the accretion rate $\dot{M}$ is an eigenvalue of the problem. Although their analysis was limited to polytropes, this important result turns out to hold in general. The first to study in some detail the emission properties of the accreting gas was Shvartsman (1971), who pointed out that the efficiency of converting gravitational potential energy into radiation was discouragingly small A full analysis of the properties of solutions in the presence of radiation was performed by Shapiro (1973a) in the optically thin case and confirmed Shvartsman's semiquantitative results: his models showed both very low luminosity and very low efficiency. Some attempts to increase the efficiency of optically thin models by including magnetic fields and dissipative processes (see, e.g., Shapiro 1973b; Mészáros 1975) were also proposed. Actually Shapiro succeeded in constructing a self-consistent model, because by considering only the optically thin regime he bypassed the major difficulty of solving the full transfer problem. On the other hand, if free-free is the dominant emission process, one can expect that an increase in $\dot{M}$ should produce also an increase in luminosity. Clearly flows with higher accretion rates are doomed to become optically thick, and this stimulated new interest in the study of solutions which contain at least an opaque core. The first attempts to solve the accretion problem treating radiation in the diffusion approximation (Tamazawa et al. 1974; Kafka & Mészáros 1976; Vitello 1978; Begelman 1979; Gillman & Stellingwerf 1980) were hindered by the apparent diverging behavior of luminosity in the inner region. It was only some years later that Flammang (1982, 1984) gave a satisfactory explanation of this pathology, pointing out that the same time that for optically thick solutions the luminosity at infinity is a further eigenvalue (see also Schmid-Burgk 1978 and Freihoffer 1981 for a discussion on relativistic transfer in spherical flows). A sequence of models of this type characterized by very high values of the accretion rate was studied by Blondin (1986). Although luminosities of optically thick solutions are higher with respect to optically thin ones, the total emitted flux is still quite low and efficiency is not improved at all by increasing $\dot{M}$.

All these investigations did not take into account, however, the effects of Comptonization, which, under certain conditions, could be important. As noted by Buff & McCray (1974) and by Ostriker et al. (1976), high-temperature radiation produced in the internal region could, in fact, heat the gas far from the hole via Compton scattering, and this, in turn, would cause internal energy to become everywhere greater than gravitational potential energy, thus inhibiting the accretion flow (see also Shull 1979). This effect places an upper bound to the possible existence of stationary solutions on the ($\log \dot{M}$, $\log L$)-plane, where L is the emitted luminosity (preheating limit). A further analysis on this subject, using a time-dependent numerical code, was performed by Cowie, Ostriker, & Stark (1978) and by Stellingwerf & Buff (1982), who reached conflicting conclusions: considering also the presence of Compton cooling, as originally suggested by Bisnovatyi-Kogan & Blinnikov (1980), Stellingwerf & Buff found, in fact, solutions in almost all the "forbidden" regions of Cowie et al.

A new class of models, in which Comptonization plays a fundamental role, was discovered by Wandel, Yahil, & Milgrom (1984); although their analysis was far from being self-consistent, it is of particular importance, since it shows for the first time that spherical accretion may also take place with high enough values of luminosity and efficiency. Actually, by increasing $\dot{M}$, optically thin (à la Shapiro) and optically thick (à la Blondin) solutions form a continuous, low-luminosity branch as discussed by Soffel (1982), while Wandel et al. solutions appear to belong to a disconnected, new branch. In a very recent work Park (1990a) presented a careful study on stationary, spherical accretion onto black holes, summarizing many aspects of the problem, and giving a definite confirmation of the existence of high-luminosity solutions, by means of a much more rigorous treatment. However, a number of important issues still remain to be clarified, such as the simultaneous determination of the two branches as solutions of a unique, self-consistent model or the effective limits imposed by Compton heating if radiation temperature is not assigned a priori but is computed together with the thermal balance of the gas. Moreover, all previous investigations contained some more or less drastic simplifications regarding a crucial aspect of the problem, that is to say, the transfer of radiation through the accreting gas. Here we present a complete analysis of stationary, accretion flows in which general relativistic radiative transfer is correctly handled using Thorne's (1981) moment formalism. Our model can be regarded as a self-consistent one in the sense that we included all the relevant physical processes that can take place in an astrophysical plasma, apart from the presence of magnetic fields and dissipative effects. The present formulation of radiative transfer allowed us to construct for the first time the whole set of accretion models, exploring all possible regimes. In a certain range of $\dot{M}$ we have found both high- and low-luminosity solutions for the same value of the accretion rate, and we show that preheating places both upper and lower bounds to the existence of high-luminosity models. Stationary, spherical accretion can therefore have a bimodal behavior, and this suggests that one of the two branches could be unstable. Although no real stability analysis was attempted, we present a simple argument, based on the minimum entropy production principle, which indicates that the high-luminosity branch might be unstable.

2. THEORY

In the following we deal with the problem of radial, stationary inflow of matter onto a Schwarzschild black hole. The hole is at rest with respect to the gas far from it, and we assume that the presence of a small magnetic field can always couple matter particles in such a way that a fluid description is adequate even in regimes where Coulomb collisions are ineffective. Both dynamical and radiative effects of magnetic fields are neglected, and dissipative processes, such as viscous heating, neutrino cooling, and particle production, are not taken into account. Moreover, we assume that electrons and ions are maintained at the same temperature by local plasma instabilities. Two-temperature models, which also include pair production, were recently computed by Park (1990b) and show essentially the same features as one-temperature models (Park 1990a), while the role played by viscous dissipation was analyzed by Turolla & Nobili (1989), and it was shown that quantitative departures from the inviscid case are not very relevant unless turbulence is almost supersonic. We consider, therefore, the accreting material as a perfect, unmagnetized, one-temperature fluid made of pure hydrogen. The hydrogen ionization state is determined both by particle-particle and by particle-photon interactions. Since we treat, at present, only the gray, i.e., frequency-integrated, radiative problem, photoionization cannot be self-consistently computed, depending on the flux of photons with energy greater than the first ionization potential of the hydrogen atom, $E_{\rm H} = 13.6$ eV. For this reason we chose to include in our models only collisional ionization, although we are aware that photoionization could be not negligible. On the other hand, Park's (1990a) models were obtained assuming that photoionization is strong enough to keep the gas fully ionized also beyond the sonic radius, and, as will be discussed in § 4, his results are quantitatively very similar to ours; such an agreement suggests that the global properties of accretion models do not depend strongly on the details of the ionization balance. The degree of collisional ionization can be computed by equating the collisional and radiative recombination rates (Buff & McCray 1974); using the interpolation by Stellingwerf & Buff (1982), it can be expressed as

$$x(T) = \frac{F}{1+F}, \qquad F = 2.0\left(\frac{T}{1\ \mathrm{K}}\right)\exp\left(-\frac{1.58\times 10^5\ \mathrm{K}}{T}\right). \tag{1}$$

Radiation is emitted by the infalling gas mainly via *e-p*, *e-e* bremsstrahlung, free-bound and bound-bound transitions. All these processes, including relativistic corrections to bremsstrahlung emission, can be described by a single cooling function,

$$\Lambda(T) = \left\{[1.42\times 10^{-27}T^{1/2}(1+4.4\times 10^{-10}T) + 6.0\times 10^{-22}T^{-1/2}]^{-1} + 10^{25}\left(\frac{T}{15{,}849\ \mathrm{K}}\right)^{-12}\right\}^{-1} \mathrm{ergs\ cm^3\ s^{-1}}. \tag{2}$$

Relation (2) was obtained by replacing in the cooling function of Stellingwerf & Buff (1982) the bremsstrahlung contribution appropriate for a mixture of hydrogen and metals with one for pure hydrogen (Novikov & Thorne 1973). We allow for both coherent (Thomson) and incoherent (Compton) electron scattering and assume that the latter can always be described by the Kompaneets equation, although repeated Compton scatterings can be treated correctly within this approximation only if electrons are nonrelativisitc, a condition that is not satisfied in some of our models. The effects induced by considering the full Boltzmann equation, which should be used if electrons are relativistic, are not easy to access but, becoming electrons mildly relativistic ($kT/m_e c^2 \lesssim 5$) only in the very inner region, we expect the Fokker-Planck approximation to give a reasonable quantitative answer.

The transfer of radiation was tackled using the projected symmetric trace-free (PSTF) (Thorne 1981) moment formalism, which is fully general relativistic and ensures a correct description of the radiation field all the way down to the hole horizon. Although this approach to radiative transfer in differentially moving media in a curved geometry is, in our opinion, the more suitable for astrophysical applications, it did not receive much attention in the past because the formalism was judged so awkward as to be no practical use. However, in the case of a

spherically symmetric, stationary spacetime, described by the line element

$$ds^2 = -\left(1 - \frac{R_g}{R}\right)c^2\,dt^2 + \left(1 - \frac{R_g}{R}\right)^{-1} dR^2 + R^2(d\theta^2 + \sin^2\theta\, d\phi^2)\,, \quad (3)$$

where $R_g = 2GM/c^2$ is the gravitational radius, the complexity of the formalism is greatly reduced. Moreover, if the flow shares the same degree of symmetry and radiative processes are isotropic in the fluid rest frame, as in the problem under examination, the gray moment equations reduce to a system of ordinary differential equations (Thorne, Flammang, & Żytkow 1981; Turolla & Nobili 1988) which govern the radial evolution of the radiation field. As in nonrelativistic transfer theory (Chandrasekhar 1960), the infinite hierarchy of equations must be truncated at a given maximum order, $l_{\max}$, specifying at the same time the closure relations for moments of order higher than $l_{\max}$. In this investigation we consider only the first two moment equations ($l = 0, 1$) for the radiation energy density $w_0 = 4\pi J$ and the radiative flux $w_1 = 4\pi H/c$, both evaluated in the fluid rest frame,

$$\begin{aligned} &w_1' - vw_0' - vw_2\left[\frac{(vy)'}{vy} - 1\right] + 2w_1\left(1 + \frac{y'}{y}\right) - \frac{4}{3}vw_0\left[\frac{(vy)'}{vy} + 2\right] = \frac{rR_g s_0}{y} \\ &w_2' - vw_1' + \frac{1}{3}w_0' + w_2\left(3 + \frac{y'}{y}\right) - 2vw_1\left[\frac{(vy)'}{vy} + 1\right] + \frac{4}{3}\frac{y'}{y}w_0 = \frac{rR_g s_1}{y}\,. \end{aligned} \quad (4)$$

Here and in the following, $r = R/R_g$ is the adimensional radial coordinate, a prime denotes differentiation with respect to $\ln r$, v is the fluid spatial velocity measured by a stationary observer in units of c, and $y = [(1 - 1/r)/(1 - v^2)]^{1/2}$. In equations (4) all moments have the dimensions of an energy density, and the radiative luminosity in the comoving frame L is related to w_1 by $L = 4\pi R^2 c w_1$. We stress that equations (4) do not contain any approximation and hold the same for v and r arbitrary close to unity. The only limitation comes from having used just two moments to describe the radiation field; this introduces an error which is typically $\sim 15\%$ in the determination of w_0 and w_1 (Turolla & Nobili 1988). The moment equations must be supplemented with a closure relating the radiation shear $w_2 = 4\pi(K - J/3)$ (see eqs. [A1] and [A2]) either to w_0 or to w_1. Usually the closure is expressed as $w_2 = f(\tau)w_0$, where τ is the electron scattering optical depth and $f(\tau)$ is the variable Eddington factor. Several different choices were proposed in the literature for f, all of them, however, discussed in connection with static atmospheres. At present we use a simple relation of the form

$$\frac{w_2}{w_1} = f(\tau) = \frac{2}{3}\frac{1}{1 + \tau^n}\,, \quad (5)$$

which can reproduce different behaviors varying the integer n; $n = 4$ was chosen in actual calculations.

The source moments s_0 and s_1 account for the energy and momentum exchange between particles and photons; by introducing the emissivity ϵ, the absorption and flux mean opacities κ_0, κ_1, and the rest-mass density ρ_0, we obtain

$$\begin{aligned} s_0 &= \rho_0(\epsilon - \kappa_0 w_0) + s_0^{\rm C}\,, \\ s_1 &= -\rho_0 \kappa_1 w_1\,. \end{aligned} \quad (6)$$

The term $s_0^{\rm C}$ arises from inelastic scatterings and can be derived by integrating over frequencies the corresponding nongray source moment (eq. [6.14] of Thorne 1981):

$$s_0^{\rm C} = \kappa_{\rm es}\rho_0 w_0 \frac{4k}{m_e c^2}(T - T_\gamma)\,; \quad (7)$$

in doing so we neglected the n^2 term in the Kompaneets equation (see Rybicki & Lightman 1979) and defined the radiation temperature

$$T_\gamma = (4k)^{-1}\int_0^\infty h\nu w_0(r, \nu)d\nu \Big/ \int_0^\infty w_0(r, \nu)d\nu \ {\rm K}\,. \quad (8)$$

Equation (7), where $\kappa_{\rm es}$ is the electron scattering opacity, yields the known result for the Compton heating-cooling of a plasma at temperature T. By assuming that emitters and absorbers are in local thermodynamic equilibrium, we can use Kirchhoff's law to write

$$s_0 = \rho_0\epsilon\left(1 - \frac{w_0}{aT^4}\right) + s_0^{\rm C} = \frac{\rho_0^2\Lambda}{m_p^2 c}\left(1 - \frac{w_0}{aT^4}\right) + s_0^{\rm C}\,. \quad (9)$$

Since in our models scattering turns out to be the dominant contribution to κ_1, we replaced the flux mean opacity with the sum of scattering and Rosseland mean opacities, the latter computed taking into account only free-free transitions:

$$\begin{aligned} \kappa_1 &\simeq \kappa_{\rm es} + \kappa_{\rm ff}^{\rm R}\,, \\ \kappa_{\rm ff}^{\rm R} &= 6.4 \times 10^{22}\rho_0 T^{-7/2}\ {\rm cm^2\ g^{-1}}\,. \end{aligned} \quad (10)$$

The equations of relativistic hydrodynamics are obtained by projecting the 4-divergence of the total (gas plus radiation) stress-energy tensor along and orthogonal to the fluid 4-velocity $\boldsymbol{u}$ and adding the rest-mass conservation. After lengthy manipulations (see Appendix for more details), they can be cast in the form

$$\begin{aligned} &(P + \rho)\frac{y'}{y} + P' + \frac{rR_g s_1}{y} = 0 \quad \text{(Euler equation)}\,, \\ &\rho' - (P + \rho)\frac{\rho_0'}{\rho_0} + \frac{rR_g s_0}{vy} = 0 \quad \text{(energy equation)}\,, \\ &\frac{(vy)'}{vy} + \frac{\rho_0'}{\rho_0} + 2 = 0 \quad \text{(continuity equation)}\,, \end{aligned} \quad (11)$$

where P and ρ are the gas pressure and energy density, including rest-mass energy, respectively. Direct integration of the continuity equation yields the baryon conservation in the familiar form

$$4\pi R^2\rho_0 yv = \dot{M}\,; \quad (12)$$

moreover, by combining equations (11), it is possible to obtain a second integral of motion (Thorne et al. 1981):

$$(1 + v^2)y^2 L - y\dot{M}\left(\frac{P + \rho}{\rho_0} + \frac{4w_0/3 + w_2}{\rho_0}\right) = \dot{E}\,. \quad (13)$$

$\dot{M}$ and $\dot{E}$ are, respectively, the accretion rate and the total luminosity, which is the sum of radiative, advective, and matter flux contributions.

By adopting yv, ρ_0, and T as independent variables, equations (11) can be written in a different form which is more suitable to numerical integration and makes presence of a critical point apparent. Once a generic set of equations of state is given, the gradients of ρ and P can be reexpressed as (Flammang 1982)

$$\frac{\rho'}{P+\rho} = A\frac{\rho_0'}{\rho_0} + B\frac{T'}{T}, \qquad \frac{P'}{P+\rho} = a\frac{\rho_0'}{\rho_0} + b\frac{T'}{T}. \tag{14}$$

where we have introduced the thermodynamical quantities

$$A = \frac{\rho_0}{P+\rho}\left(\frac{\partial\rho}{\partial\rho_0}\right)_T, \quad B = \frac{T}{P+\rho}\left(\frac{\partial\rho}{\partial T}\right)_{\rho_0},$$
$$a = \frac{\rho_0}{P+\rho}\left(\frac{\partial P}{\partial\rho_0}\right)_T, \quad b = \frac{T}{P+\rho}\left(\frac{\partial P}{\partial T}\right)_{\rho_0};$$

from the reciprocity relation it follows that $A + b = 1$. By inserting equations (14) in equations (11) and recalling the definition of y, we finally get

$$(v^2 - v_s^2)\frac{(yv)'}{yv} - 2v_s^2 + \frac{1}{2y^2 r} + \frac{rR_g}{yv(P+\rho)}[(\Gamma-1)s_0 + vs_1] = 0,$$
$$\frac{T'}{T} - (\Gamma-1)\frac{\rho_0'}{\rho_0} - \frac{rR_g s_0}{Bvy(P+\rho)} = 0, \tag{15}$$
$$\frac{(vy)'}{vy} + \frac{\rho_0'}{\rho_0} + 2 = 0,$$

where $\Gamma = 1 + b/B$ is the local adiabatic exponent and $v_s^2 \equiv (\partial P/\partial\rho)_s = a + b^2/B$ is the adiabatic sound speed squared. As can be seen from the first of equations (15), the hydrodynamical equations exhibit a critical point which coincides with the sonic point where the flow velocity equals the matter sound speed.

Since the temperature range spanned by typical accretion models is such that hydrogen is neutral far from the hole and electrons may become relativistic near the horizon, the equations of state must incorporate both the effects of ionization and the contribution of relativistic electrons. As long as protons are nonrelativistic, their expression is

$$P = (1+x)\frac{\rho_0}{m_p}kT,$$
$$\rho = \rho_0 c^2 + \frac{3}{2}(x+x^*)\frac{\rho_0}{m_p}kT + (1-x)\frac{\rho_0}{m_p}E_H; \tag{16}$$

here

$$x^* = \frac{2}{3}[\theta^{-1}(\eta-1) - 1], \quad \theta = \frac{kT}{m_e c^2}, \quad \eta = \frac{K_3(\theta^{-1})}{K_2(\theta^{-1})},$$

and K_n is the modified Bessel function of order n. The relativistic correction for electrons is contained in x^*, while x, given by equation (1), accounts for the varying degree of ionization. Starting from equations (16), it is now possible to compute all thermodynamical quantities of interest, like v_s^2 and Γ; the polynomial fit by Service (1986) was used to evaluate x^*.

Equations (4) and (15), together with the gas constituent equations (16) and the expressions for the source moments (6), describe stationary, spherical accretion onto a Schwarzschild hole in a self-consistent way, within the hypothesis stated up to now. It should be noted, however, that the radiation temperature T_γ can be computed only if the frequency-dependent transfer is solved, being defined as an integral over the actual spectral distribution of the photon energy density. A correct determination of T_γ is of key importance in understanding the physical properties of accretion and is still one of the major difficulties in the framework of gray models. A reasonable way out of this problem was recently proposed by Park & Ostriker (1989) and Park (1990a), who estimated the energy exchange due to repeated Compton scatterings between a thermal, nonrelativistic electron gas and the radiation field. Following their approach, we assume that the radiation temperature is governed by the equation

$$\frac{T_\gamma'}{T_\gamma} = Y_C\frac{T - T_\gamma}{T}, \tag{17}$$

where $Y_C = 4kT\max(\tau, \tau^2)/m_e c^2$ is the Compton parameter.

3. CRITICAL POINTS AND BOUNDARY CONDITIONS

The accreting flow and the radiation field generated by the infalling gas are described by the radiative transfer and hydrodynamical equations, equations (4) and (15), coupled to the radiation temperature equation (17) and supplemented by the constituent relations (6) and (16). The resulting system is formed by 6 differential equations in the 6 unknown functions w_0, w_1, yv, ρ_0, T, and T_γ which have to be integrated subject to suitable boundary conditions. As is well known and discussed in the previous section, stationary, spherical flows possess a critical point at $v = v_s$, where a regularly condition must be imposed if the solution has to be transonic. Not so evident, and far less appreciated, is the presence of a second critical point which appears in the moment equations. This singular point can be made explicit by solving equations (4) with respect to either w_0' or w_1' and substituting for w_2 the closure (5). After some manipulation they take the form

$$(v^2 - vf - \tfrac{1}{3})w_l' = G_l(r, w_0, w_1, v, v'), \quad l = 0, 1, \tag{18}$$

which shows that whenever

$$v^2 - vf - \tfrac{1}{3} = 0, \tag{19}$$

equations (4) develop a singularity. The existence of singular points in stationary, spherically symmetric moment equations was realized and discussed in detail by Turolla & Nobili (1988), who proved that, for a generic truncation order l_{max}, there exist $l_{max} + 1$ critical points located where the Legendre polynomial $P_{l_{max}+1}(v)$ vanishes; in the present case $l_{max} = 1$ and $P_2 = 3(v^2 - \frac{1}{3})/2$ is, in fact, proportional to the coefficient of moments derivatives in equation (18), apart from the term vf: this difference arises because they assumed a closure in which w_2 is a known function of r, not related to moments of lower order. In the accretion problem only the positive root of equation (19) is meaningful, so just one critical point is to be expected, and its location depends on the actual value of $f(\tau)$. Similarly to what happens in the case of the hydrodynamical critical point, a regularity condition must be imposed at the radius where the value of the flow velocity satisfies equation (19). For optically thick flows ($f \to 0$) the singularity appears at $v = 3^{-1/2}$ and then moves toward higher values of v with decreasing optical

depth, until it reaches $v = 1$ in the optically thin regime where $f \to \frac{2}{3}$. In the latter case the regularity condition becomes a boundary condition for the radiation moments at the horizon. It can be proved that the generalization of equation (19) to an arbitrary truncation order is

$$P_{l_{\max}+1}(v) - \frac{2l_{\max}+1}{l_{\max}+1} f(\tau) P_{l_{\max}}(v) = 0 ,$$

where now $f(\tau) = w_{l_{\max}+1}/w_{l_{\max}}$. The requirement for a regular behavior of the solutions at the critical points reduces by 2 the number of boundary conditions that have to be imposed to solve the complete system of differential equations (4), (15), and (17). The exact form of such regularity conditions will be discussed later on.

As far as boundary conditions are concerned, we note that the particular nature of the problem requires their specification both at radial infinity and at the horizon. In particular, in the hydrostatic region outside the sonic radius the gas must be in radiative energy equilibrium, a condition which translates into $s_0 = 0$. Since the density gradient vanishes there, it follows from the energy equation that the natural boundary condition for T at radial infinity is

$$\frac{T'}{T} = 0 . \tag{20}$$

At the same time we have to require that for $r \to \infty$ the radiation field streams radially, that is to say, $w_0 = w_1 \propto r^{-2}$, or, equivalently,

$$\frac{w_0'}{w_0} = -2 ; \tag{21}$$

equation (21) is the Sommerfeld radiative condition and holds if matter far from the hole is not illuminated by an external source.

The form of the boundary condition for the radiation temperature is a more delicate issue. Park (1990a) imposed either $T_\gamma = T$ or $T_\gamma = T/4$ at the horizon, depending on the value of the Compton parameter there. If $Y_C \gg 1$, Compton scattering is effective in establishing thermal equilibrium between matter and radiation, while in the opposite case the radiation spectrum remains a pure bremsstrahlung, characterized by $T_\gamma = T/4$. Actually, in the context of gray accretion models, the concept itself of radiation temperature is introduced only to evaluate the Compton energy exchange between electrons and photons and become meaningless if Comptonization is ineffective. For this reason we choose to use

$$T_\gamma = T , \tag{22}$$

independent of the value of Y_C at $r = 1$.

The last condition is used, then, to fix the value of the matter density at some radius, this being the only degree of freedom of the model. In particular, we assigned ρ_0 at the horizon:

$$\rho_0 = (\rho_0)_H ; \tag{23}$$

clearly condition (23) is completely equivalent to fixing the accretion rate $\dot{M}$.

The numerical integration of the system of differential equations (4), (15), and (17), subject to boundary conditions (20)–(23) and to regularity conditions at the two critical points, was performed using a generalized Henyey method (Nobili & Turolla 1988). The main advantage of this relaxation-type technique is that critical-point conditions can be handled on the same footing as boundary conditions and need not to be specified with much accuracy, in the sense that any reasonable condition which forces the solution to cross the critical points with bounded derivative is usually enough to guarantee the convergence of the numerical scheme. In the present case we imposed

$$\frac{(yv)'}{yv} = -1 \tag{24}$$

at the sonic point, since the 4-velocity logarithmic gradient switches from -2 (hydrostatic region) to $-\frac{1}{2}$ (free-free region) just around the sonic radius. The second regularity constraint is provided by the request that either $w_0 \propto \tau w_1/y$ or $w_0 \propto r^{-2}$ at the radius where expression (19) vanishes, if $\tau \gtrsim 1$ or $\tau < 1$, respectively (see Turolla & Nobili 1988); written in terms of logarithmic derivatives, the two conditions become

$$\frac{w_0'}{w_0} = \frac{w_1'}{w_1} + \frac{\tau'}{\tau} - \frac{y'}{y} , \qquad \frac{w_0'}{w_0} = -2 . \tag{25}$$

The location of the critical points is automatically found by the code, looking for the radii where the Jacobian of the system of differential equations vanishes. The electron scattering optical depth, needed to evaluate the first of equations (25) and the function $f(\tau)$, was computed replacing $\int_\infty^R \kappa_{es}\rho_0\, dR$ with a discrete sum over the intervals into which the integration domain is divided. Starting from the trial solution, all quantities, including both the optical depth and the Jacobian, are then upgraded as convergence proceeds. Logarithmic variables were actually used apart from radiation moments; the latter were replaced by new variables proportional to $r^2 w_l$. The CPU time for generating a model was typically ~ 5 minutes on a VAX 8600.

Finally we note that the differential form of the continuity equation can be replaced with the first integral (12), assigning $\dot{M}$ instead of $(\rho_0)_H$. We preferred the former choice, however, in order to provide a further accuracy check on our numerical results by looking at the constancy of the accretion rate along the solution. In principle the same considerations can be applied to the energy equation, which can be replaced by the integral (13). There are, however, two major drawbacks in this case: $\dot{M}$ and $\dot{E}$ are related to each other, but this relation is not a priori known, and moreover equation (13) is so awkward numerically as to be of little practical use. In actual models, in fact, $\dot{M}$ was found to be constant up to few parts in 10^5, while the fractional variation of $\dot{E}$ can be as high as 4%.

4. NUMERICAL MODELS AND DISCUSSION

In this section we present the results of numerical integration of the coupled flow and radiative transfer equations. We constructed accretion models characterized by a density at the horizon in the range $5.0 \times 10^{-8} < (\rho_0)_H < 2.5 \times 10^{-4}$, corresponding to $0.03 \lesssim \dot{m} \lesssim 200$; here $\dot{m} = \dot{M}/\dot{M}_{\rm Edd}$, being $\dot{M}_{\rm Edd} = L_{\rm Edd}/c^2$, the Eddington accretion rate. In all cases the radial coordinate spans the range $1 < r < 10^{10}$, and 130 mesh points are used, equally spaced on a logarithmic scale; the fractional accuracy of the solution is less than 10^{-3}, this being the largest fractional correction on variables at the final iteration. Our results depend on the hole mass at least when bremsstrahlung absorption, which is not scale-free (Chang & Ostriker 1985), becomes important; at present a reasonable value for a stellar mass hole was chosen, $M = 3\ M_\odot$. The

TABLE 1

CHARACTERISTIC PARAMETERS FOR SELECTED MODELS ALONG THE LOW-LUMINOSITY BRANCH

$(\rho_0)_H$ (g cm^{-3})	$\dot{m}$	l	$e = l/\dot{m}$	$(\rho_0)_H$ (g cm^{-3})	$\dot{m}$	l	$e = l/\dot{m}$
5×10^{-8}	0.035	3.0×10^{-8}	8.6×10^{-7}	4×10^{-6}	2.85	4.4×10^{-7}	1.5×10^{-7}
1×10^{-7}	0.071	3.5×10^{-8}	4.9×10^{-7}	6×10^{-6}	4.27	9.2×10^{-7}	2.2×10^{-7}
1.3×10^{-7}	0.092	2.5×10^{-8}	2.7×10^{-7}	1×10^{-5}	7.12	1.5×10^{-6}	2.1×10^{-7}
1.7×10^{-7}	0.12	1.1×10^{-8}	9.4×10^{-8}	4×10^{-5}	28.5	4.8×10^{-6}	1.7×10^{-7}
2×10^{-7}	0.14	1.4×10^{-8}	9.7×10^{-8}	6×10^{-5}	42.7	6.6×10^{-6}	1.6×10^{-7}
5×10^{-7}	0.36	3.5×10^{-8}	9.8×10^{-8}	1×10^{-4}	71.2	8.8×10^{-6}	1.2×10^{-7}
1×10^{-6}	0.71	7.6×10^{-8}	1.1×10^{-7}	2.5×10^{-4}	178	1.5×10^{-5}	8.4×10^{-8}

TABLE 2

CHARACTERISTIC PARAMETERS FOR SELECTED MODELS ALONG THE HIGH-LUMINOSITY BRANCH

$(\rho_0)_H$ (g cm^{-3})	$\dot{m}$	l	$e = l/\dot{m}$	$\log (T_\gamma)_\infty$	$(\rho_0)_H$ (g cm^{-3})	$\dot{m}$	l	$e = l/\dot{m}$	$\log (T_\gamma)_\infty$
3.7×10^{-6}	2.51	2.0×10^{-4}	8.2×10^{-5}	9.3	2×10^{-5}	14.1	7.7×10^{-4}	5.5×10^{-5}	8.6
4×10^{-6}	2.85	2.1×10^{-4}	7.3×10^{-5}	9.3	4×10^{-5}	28.5	1.8×10^{-3}	6.4×10^{-5}	8.3
6×10^{-6}	4.27	2.7×10^{-4}	6.4×10^{-5}	9.2	6×10^{-5}	42.7	3.5×10^{-3}	8.1×10^{-5}	8.2
8×10^{-6}	5.55	3.4×10^{-4}	6.2×10^{-5}	9.0	8×10^{-5}	55.5	5.9×10^{-3}	1.1×10^{-4}	8.1
1.1×10^{-5}	7.68	4.5×10^{-4}	5.9×10^{-5}	8.9	1×10^{-4}	71.2	9.4×10^{-3}	1.3×10^{-4}	8.1
1.5×10^{-5}	10.5	5.9×10^{-4}	5.6×10^{-5}	8.8	1.3×10^{-4}	91.6	1.9×10^{-2}	2.1×10^{-4}	8.1

values of some characteristic parameters of selected models are summarized in Tables 1 and 2, where $l = L/L_{\rm Edd}$ is the luminosity in units of the Eddington luminosity and the efficiency $e = l/\dot{m}$ has been introduced. Figure 1 shows the position of our solutions in the (log $\dot{m}$, log l)-plane (*crosses*), where some models of Park (1990a) (*open triangles*) are also shown for comparison. From the figure there appears the existence of two separated branches with very different emission properties: a low-luminosity (LL) and a high-luminosity (HL) branch. Our HL models are in good agreement with those of Wandel et al. (1984) and Park (1990a), who first proved the existence of high-luminosity solutions. Although the possible presence of two distinct accretion regimes characterized by the same value of the accretion rate was already realized by Park (1990a), the simultaneous determination of both the branches within the framework of a unique, self-consistent model of accretion is here presented for the first time.

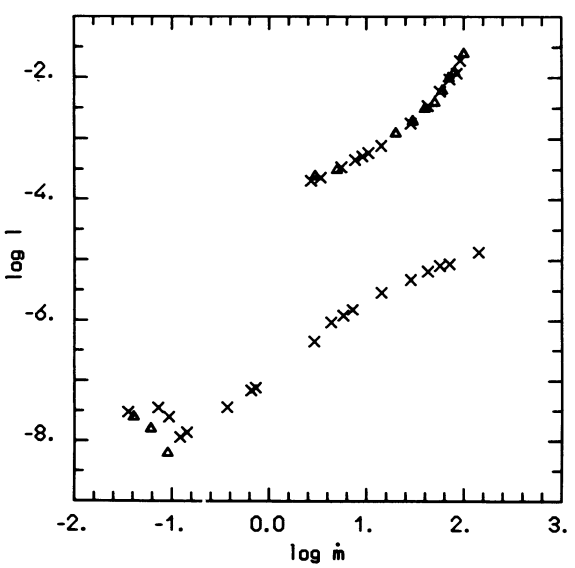

FIG. 1.—The (log $\dot{m}$, log l)-diagram for our solutions (*crosses*); some of Park's (1990a) models (*open triangles*) are also shown for comparison.

In the following we briefly discuss the main properties of our accretion models. In this respect it is useful to introduce the effective optical depth, $\tau_{\rm eff} = [3\tau_{\rm P}(\tau + \tau_{\rm R})]^{1/2}$, where $\tau_{\rm P}$ and $\tau_{\rm R}$ are the optical depths computed using Planck and Rosseland mean opacities, respectively. In all our models the temperature at radial infinity is close to 10^4 K, the value at which radiative energy equilibrium is attained when free-bound cooling dominates; we stress that this particular value for T_∞ was not imposed "a priori" but is a natural consequence of boundary condition (20). For low $\dot{m}$, $\dot{m} \sim 0.035$, models are optically thin and show the distinctive features of Shapiro's (1973a) solutions: adiabatic temperature profile interior to the sonic radius, electrons becoming relativistic near the horizon where $T \sim 10^{10}$ K, hypersonic and completely ionized flow, no Comptonization, and radial streaming of the radiation field. The run of variables for a typical model of this class is plotted in Figure 2. As $\dot{m}$ increases up to $\sim$0.1, the external region becomes more and more isothermal because of the increasing efficiency of cooling processes; this in turn drives a decrease of the temperature in the inner region and hence of the total luminosity, which reaches a local minimum (Soffel 1982; Park 1990a). Around $\dot{m} \sim 0.1$ bremmstrahlung absorption is no longer negligible, and models start to become effectively optically thick near the horizon. The quantitative difference of our solutions with respect to those of Park in this region (see Fig. 1) most likely arises because he did not include true absorption in his calculations. For the same reason, Park could not find numerical solutions in the range $0.1 \lesssim \dot{m} \lesssim 3$, where models form an optically thick core. Now the temperature profile is almost isothermal everywhere at $T \sim 10^4$ K, apart from the inner region where $\tau_{\rm eff} \gtrsim 1$ and heating exceeds cooling (Fig. 3); the temperature at the horizon is, however, much smaller with respect to the optically thin case. When the internal region becomes thick, matter and radiation approach equilibrium ($w_0 \sim aT^4$; again see Fig. 3), and an increase in $\dot{m}$

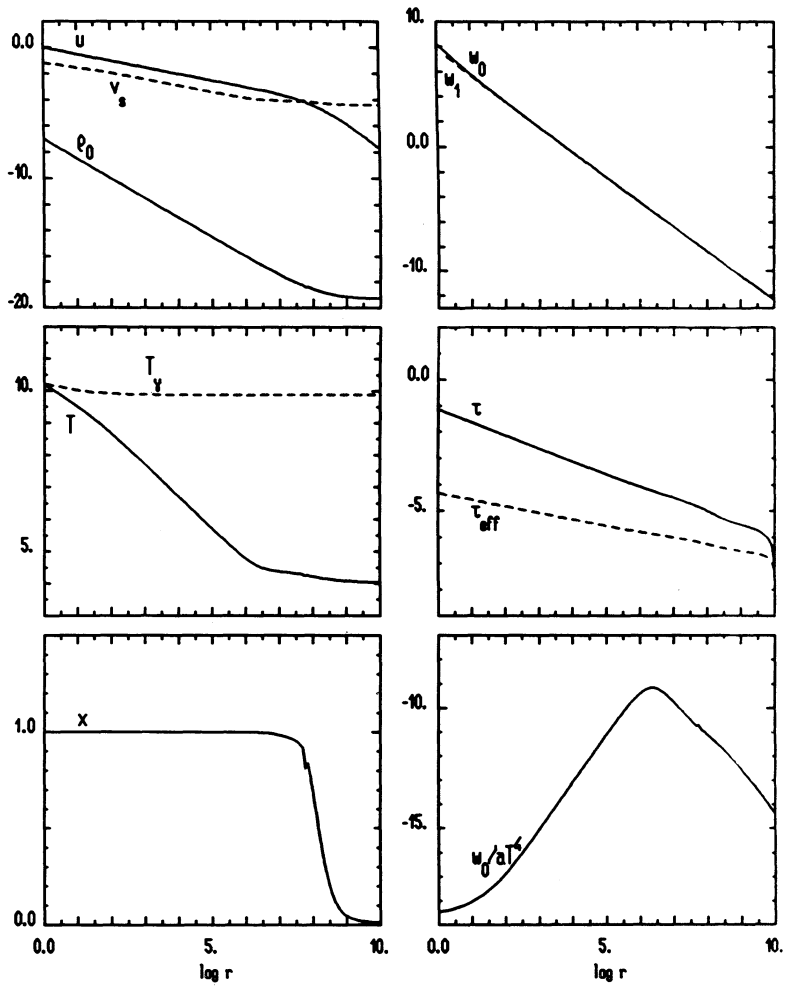

FIG. 2.—*Top left to bottom right:* the run of 4-velocity $u = yv$, sound speed v_s, and matter density ρ_0; radiation energy density w_0 and radiation flux w_1, both in ergs cm^{-3}; gas and radiation temperatures, T and T_γ; electron scattering and effective optical depths, τ and $\tau_{\rm eff}$; ionization degree x; and the ratio w_0/aT^4. Here $(\rho_0)_H = 1 \times 10^{-7}$ g cm^{-3}, $\dot{m} = 0.071$.

again produces an increase in luminosity. With increasing $\dot{m}$ the effective optical depth becomes higher and higher and the core starts to be thick also for electron scattering. As a consequence a trapping radius does form, below which photons are dragged into the hole, and the rise in luminosity becomes slower. For $\dot{m} \gtrsim 3$ the models are similar to Blondin's (1986) hypercritical solutions and exhibit a thermalized, diffusive core with $w_0 \simeq aT^4$, $3w_1 \simeq yw_0/\tau$; Comptonization is still negligible everywhere, and the flow is hypersonic with a wide region of partial ionization. An example of such a solution is shown in Figure 4. Introducing the thermalization radius $r_{\rm th}$, where w_0 starts to equal aT^4, any increase in luminosity requires a corresponding increase in $r_{\rm th}$, as can be seen by comparing Figures 3 and 4, since optically thick models radiate a luminosity $L = 4\pi R_{\rm th}^2 \sigma T(R_{\rm th})^4$. The emergent radiation spectrum should be almost exactly blackbody because the last scattering radius is always smaller than $r_{\rm th}$, and the infall velocity of the emitting photosphere is ~ 0.01 or less, so that Comptonization due to both bulk and thermal motions is negligible (Blandford & Payne 1981; Payne & Blandford 1981; Colpi 1988).[1]

[1] Preliminary results of frequency-dependent calculations show, however, that the emergent spectrum could be significantly different from a pure blackbody, owing to bremsstrahlung emission in the outer layers.

High-luminosity solutions are characterized by a much more complex thermal behavior in which Comptonization plays a fundamental role, as first noted by Wandel et al. (1984). These models are effectively optically thin, becoming marginally thick only for $\dot{m} \sim 70$, although they always contain an inner region which is optically thick to scattering. Free-bound cooling still dominates the outer region, keeping temperature close to $\sim 10^4$ K until Compton heating overwhelms cooling, producing a sudden increase in T around $r_{\rm st} = 10^{4.5}$–$10^{5.5}$, the exact location depending on $\dot{m}$. Temperature must reach a value between 10^6 and 10^7 K before bremsstrahlung cooling becomes competitive, after which a (pseudo-)adiabatic regime is established, as discussed by Wandel et al. and Park. In the inner region, which is truly adiabatic, electrons are mildly relativistic and Comptonization succeeds in maintaining matter and radiation in thermal equilibrium. Figures 5 and 6 show the run of variables for two models of the high-luminosity (HL) branch. Hydrogen becomes completely ionized for $r < r_{\rm st}$, while it is only partially ionized outside, where the sonic point is located. The Mach number never gets much greater than unity, owing to the high value of the sound speed, and reaches a minimum around $r_{\rm st}$. For $\dot{m} < 70$, $w_0 < aT^4$ at any radius, while models with higher $\dot{m}$ do have a thermalization radius $r_{\rm th}$ where $w_0 = aT^4$. Numerical integration of all HL models

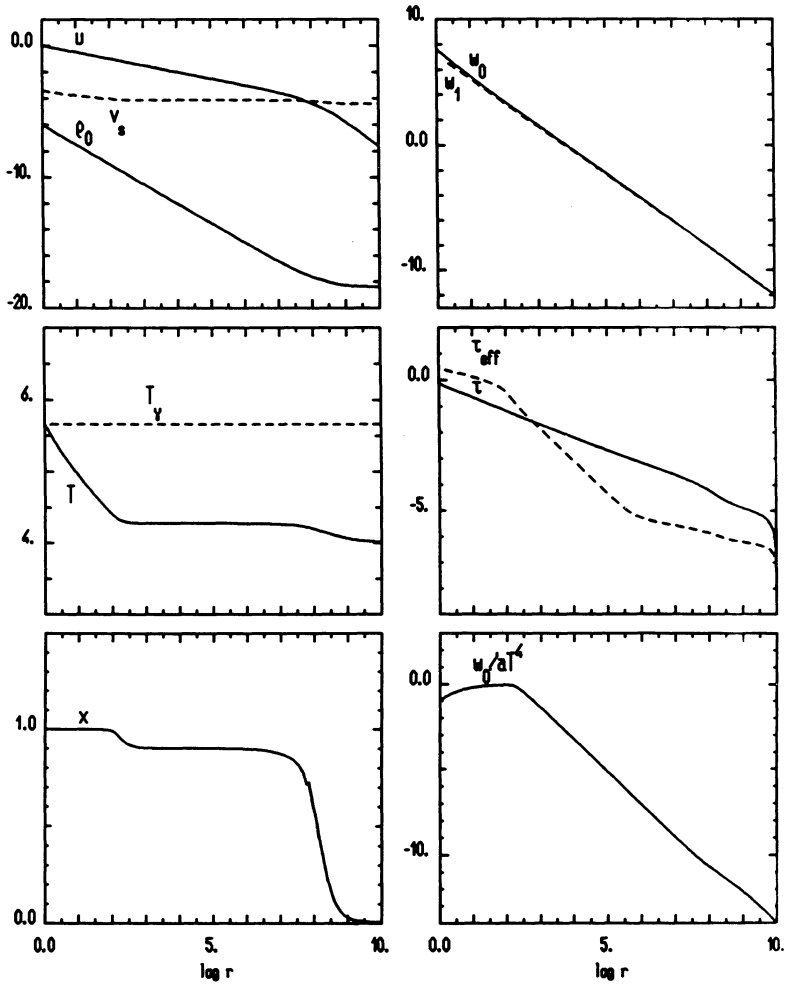

FIG. 3.—Same as Fig. 2, but for the $(\rho_0)_H = 1 \times 10^{-6}$ g cm^{-3}, $\dot{m} = 0.71$ model

proved rather troublesome, and we were forced to use a finer grid around r_{st}, inserting ~ 40 new mesh points, to avoid problems connected with the steep temperature gradient there.

As we have seen, low-temperature, optically thick models are expected to emit blackbody radiation from a photosphere of radius r_{th} at an effective temperature $\approx 10^4$ K. It is interesting to note that the most luminous HL solutions, which are characterized by very different physical properties, could turn out to be quite indistinguishable from low-luminosity (LL) models with the same $\dot{m}$ for a distant observer. Radiation, mostly produced in the inner region and strongly Comptonized, is in fact reprocessed by outer layers that have higher and higher true opacity owing to decreasing temperature, and is progressively thermalized until LTE is reached at r_{th} (Fig. 6). The emergent spectrum should again be blackbody, since the effective temperature at r_{th} coincides with the matter temperature at the same radius, $T \sim 4 \times 10^4$ K, as can be easily verified by a direct calculation. As seen from infinity, accretion onto a black hole with $\dot{m} \gtrsim 70$ will therefore have the same observational appearance irrespective of the details of the process, apart from the luminosity produced, which is about 1000 times greater along the HL branch. This large variation in the energy output can be interpreted in terms of the different thermalization radii of the two solutions; for example, the $\dot{m} = 71$ models have $(r_{th})_{HL} \sim 15(r_{th})_{LL}$, while the effective temperatures are almost equal. The old suggestion by Shvartsman (1971) that isolated, accreting holes should appear similar to DC white dwarfs seems therefore to be put on a firmer footing by our analysis. All these considerations do not hold, however, for HL models with $\dot{m} < 70$ that have only a scattering but no thermalization radius because of lower density and higher temperatures; in this case the properties of the emitted radiation are very different and should show the features of a superposition of Comptonized bremsstrahlung spectra at different temperatures.

As already noted by Park, the HL branch is not smoothly connected to the LL branch, and HL solutions seem to exist only for $2 \lesssim \dot{m} \lesssim 100$ (again see Fig. 1). It was realized long ago by Ostriker and coworkers (Ostriker et al. 1976; Cowie et al. 1978) that if Comptonization is very efficient, high-energy photons generated in the inner region can heat up the gas around the accretion radius to the point at which matter internal energy becomes greater than gravitational potential energy, thus inhibiting a sonic transition (preheating effect); if this condition is satisfied, no stationary flow can exist. The most natural explanation of the nonexistence of models with very high radiation temperature should therefore be sought in terms of preheating effects. From the first of equations (15) it is

possible to derive an implicit expression for the sonic radius r_s,

$$r_s = \frac{1}{4y^2 v_s^2}\left\{1 + \frac{2r_s^2 R_g}{y v_s h \rho_0 c^2}\left[(\Gamma - 1)s_0 + v_s s_1\right]\right\}, \quad (26)$$

where $h = (P + \rho)/\rho_0 c^2$ is the (adimensional) enthalpy per unit mass. Since in all models the sonic point is well within the region where radiation streams radially, we can put $w_0 = w_1 = L/4\pi R^2 c$ in equation (26), obtaining

$$r_s = \frac{1}{4y^2 v_s^2}\left\{1 + (\Gamma - 1)\frac{\rho_0 y r^2 R_g}{v_s h c^2}\frac{\Lambda}{m_p^2 c} + \frac{yl}{h}\left[\frac{4}{v_s}\frac{kT}{m_e c^2}(\Gamma - 1)\left(1 - \frac{T_\gamma}{T}\right) - 1\right]\right\}. \quad (27)$$

The requirement that r_s be positive leads to the "classical" result for the preheating limit,

$$1 + (\Gamma - 1)\frac{\Lambda}{2\kappa_{es} m_p^2 c^3 v_s^2}\dot{m} + \left[\frac{\Gamma - 1}{v_s}\frac{4kT}{m_e c^2}\left(1 - \frac{T_\gamma}{T}\right) - 1\right] l = 0, \quad (28)$$

where we assumed $y = h = 1$; in both equation (27) and equation (28) true absorption was neglected. However, besides the limit given by equation (28), a further condition must be satisfied in order to avoid the appearance of a second sonic point, which will be catastrophic, since there is no free parameter left that can be adjusted to make this new sonic transition smooth. Interior to the sonic radius gravity prevails and the flow is practically in free fall. The only effect that could produce a deviation from free fall is a sharp enhancement of the gas internal energy, as can be easily seen by computing the logarithmic rate of change of the velocity gradient $D \equiv (yv)'/(yv)$ starting from the first of equations (15),

$$\frac{\delta \ln |D|}{\delta \ln v_s^2} = \frac{v_s^2}{v^2 - v_s^2}\frac{2 + D}{D}. \quad (29)$$

Since the right-hand side of equation (29) is always negative, because, for $r < r_s$, v is greater than v_s, D is negative, and $2 + D = -\rho_0'/\rho_0 > 0$, any increase of the sound speed, that is to say, of matter energy, produces a flattening of the velocity profile which becomes pronounced as v_s approaches v. Moreover, under such conditions, the rise of the sound speed cannot be stopped by any modification in the flow dynamics, depending almost entirely upon radiative heating-cooling balance, so that a second sonic transition would be unavoidable. Station-

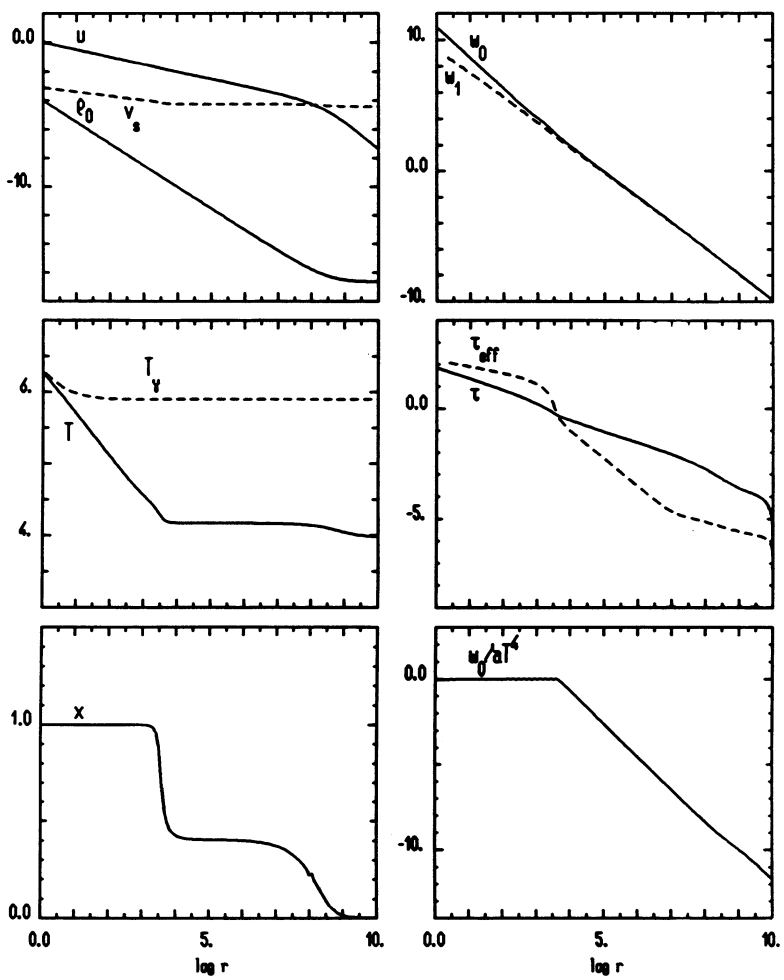

FIG. 4.—Same as Fig. 2, but for the $(\rho_0)_H = 1 \times 10^{-4}$ g cm^{-3}, $m = 71$, low-luminosity model

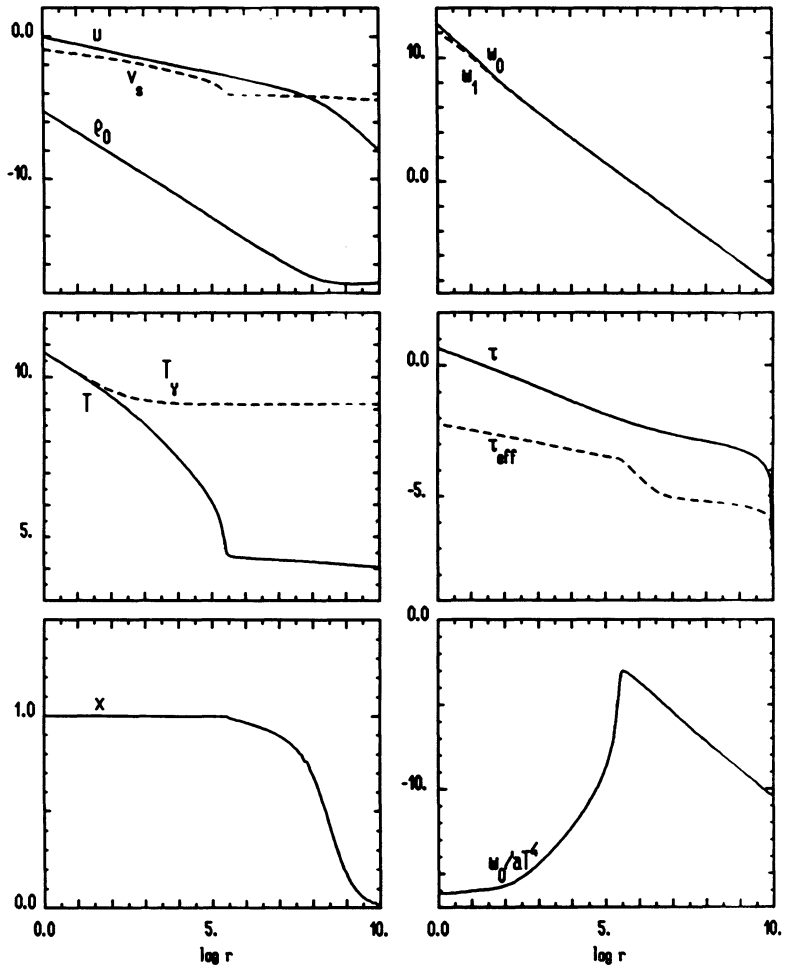

FIG. 5.—Same as Fig. 2, but for the $(\rho_0)_H = 6 \times 10^{-6}$ g cm^{-3}, $\dot{m} = 4.27$, high-luminosity model

ary, regular solutions exist, therefore, only if heating inside the sonic point is not so drastic as to produce an excess of internal with respect to gravitational energy, as was discussed by Cowie et al. in connection with time-dependent models. All previous considerations can be put on a more quantitative ground by assuming that $D \leq 0$ represents a safe condition for the existence of solutions. From the first of equations (15), this amounts to asking that

$$2v_s^2 - \frac{1}{2y^2 r} - \frac{rR_g}{yv(P+\rho)}\left[(\Gamma - 1)s_0 + vs_1\right] \leq 0 \qquad (30)$$

for $r \leq r_s$. As was discussed, HL models show a steepening of the temperature profile at r_{st} where the gas internal energy sharply rises; condition (30) should therefore be checked there. For typical values of r_{st}, radiation streams radially, $y = h = 1$, $v \ll kT_\gamma/m_e c^2$, $v_s^2 \ll 1/r$, and we can neglect bremsstrahlung emission and absorption with respect to Compton heating. With these simplifications the limit implied by equation (30) can be written as

$$2\kappa_{es}\rho_0 r_{st}^2 R_g(\Gamma - 1)\frac{4kT_\gamma}{m_e c^2} l - \dot{m} = 0 \,. \qquad (31)$$

Both equations (28) and (31) are represented by a curve in the (log $\dot{m}$, log l)-plane, which is an upper bound to the existence of regular solutions; it should be noted that they are not necessarily linear relations between $\dot{m}$ and l because all quantities, in particular T_γ, entering equations (28) and (31) depend on the accretion rate. We have computed the two limits for each HL model using the actual values of all variables at r_s and r_{st}. The result is shown in Figure 7, where the curve a denotes the "classical" preheating limit (eq. [28]) and curve b the limit given by equation (31). Both these curves were obtained by a polynomial fit to single points; the result was extrapolated to visualize better the behavior of equations (28) and (31) outside the explored range of $\dot{m}$. The shaded area in the picture is the forbidden region where no stationary, regular solution to the present model of accretion can be found. As can be seen from Figure 7, the solution with the lowest $\dot{m}$, $\dot{m} = 2.51$, lies very close to the "classical" preheating limit, while that with the highest accretion rate, $\dot{m} = 91.6$, is near the "generalized" preheating limit; the better agreement at low $\dot{m}$ is quite naturally interpreted as due to the rather steep behavior of both equation (31) and the $\dot{m}$-l relation at high $\dot{m}$. The previous finding of Park, confirmed by our results, that HL solutions exist only in a limited interval of accretion rates can therefore be explained in terms of the twofold action of the preheating effect. On one side, solutions with $\dot{m} \lesssim 2$ cannot exist because of too high a radiation temperature, which produces an overheating of the gas around the accretion radius; on the other side, the presence

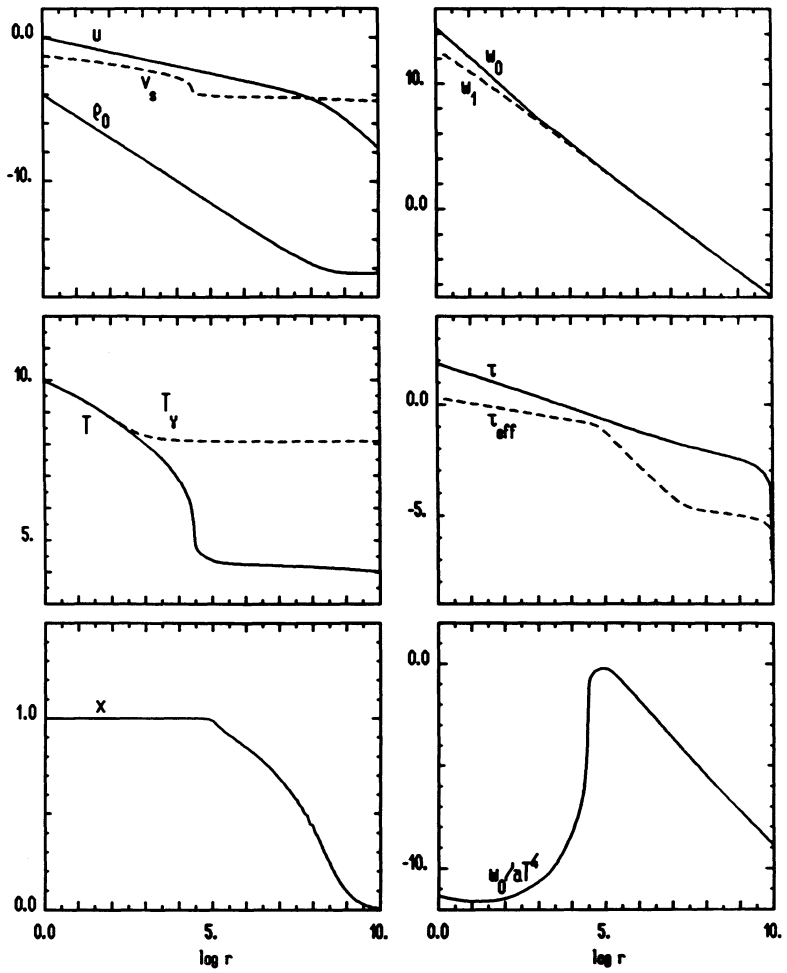

FIG. 6.—Same as Fig. 2, but for the $(\rho_0)_H = 1 \times 10^{-4}$ g cm^{-3}, $\dot{m} = 71$, high-luminosity model

of models with $\dot{m} \gtrsim 100$ is forbidden by the high radiation flux combined with an increasing scattering optical depth which makes Compton heating more and more effective interior to the sonic radius. We note once again that all previous considerations apply only to regular solutions, while flows which develop a shock transition are not necessarily limited by preheating effects. The possible existence of such solutions was explored by Chang & Ostriker (1985), who actually found that stationary shocks can form in accreting flows. Shocked solutions seem very promising owing to their high efficiency and luminosity, but their appearance still needs confirmation within a self-consistent accretion model. Our numerical code can handle standing shocks using relativistic Rankine-Hugoniot jump conditions, but, despite an intensive search, we were not able to find any shocked solution, at least near the low end of the HL branch where the flow seems naturally on the edge of forming a shock; models with $\dot{m} \sim 3$ show, in fact, a deep minimum around r_{st} in the Mach number where the ratio v/v_s gets extremely close to 1.

A major open question remains the stability of solutions, and in particular of those along the HL branch. The bimodal pattern of accretion models for $\dot{m} \gtrsim 2$ suggests, in fact, that at least one of the branches could be unstable. If proved to be true, such a possibility would be of extreme interest in connection with the theoretical interpretation of phenomena like

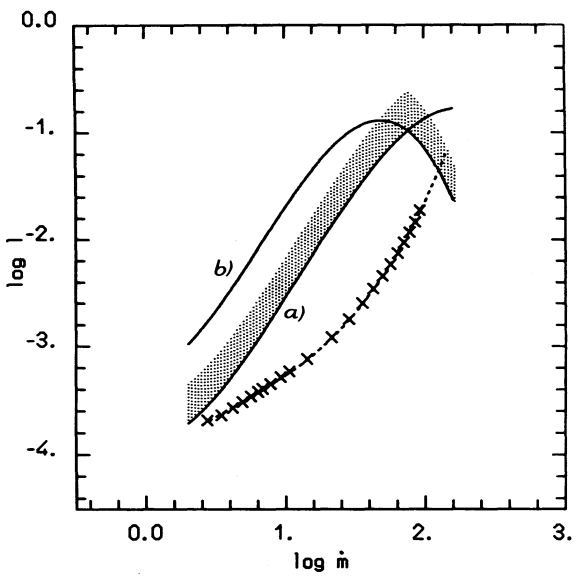

FIG. 7.—The (log $\dot{m}$, log l)-diagram for the HL solutions; curve *a* marks the "classical" and curve *b* the "generalized" preheating limits. The shaded area is the forbidden region where no stationary solution can be found (see text for details).

flaring emission from compact objects. In the past, several investigations (see, e.g., Stellingwerf & Buff 1978; Moncrief 1980; Gilden & Wheeler 1980; Vitello 1984) were devoted to the stability analysis of spherical flows under special assumptions; even if no definite conclusion can be reached in the case of the self-consistent accretion model considered here, several clues seem to indicate that LL models should indeed be stable. Both optically thin and optically thick solutions are, in fact, almost adiabatic, while models with $\dot{m} \sim 1$ are nearly isothermal, and the stability of such regimes was proved by Moncrief (1980) and by Stellingwerf & Buff (1978), respectively. None of these considerations can actually be applied to HL models, and although no thorough stability analysis will be attempted here, we present a simple argument supporting the idea that HL solutions might be unstable. According to Prigogine's criterion, the steady state (when it exists) is characterized by the minimum rate of entropy production. Nobili, Calvani, & Turolla (1985) suggested that when several stationary solutions exist, the stable steady state might be the one with the minimum rate of entropy production among them. Actually, an application of the minimum entropy production criterion to radiation hydrodynamics is a delicate issue because photons can be quite far away from thermodynamical equilibrium even if matter is always near to it (see Essex 1984 for a complete discussion). If we assume, nevertheless, that in the present case the conditions for the validity of Prigogine's criterion are fulfilled and follow the original idea of Nobili et al., the stability of solutions can be tested evaluating the entropy production rate for each model along the two branches and comparing the results. For a non–perfect fluid characterized by a heat flux 4-vector q^i and by a shear viscosity coefficient η, the entropy generated per unit volume and per unit time is (Novikov & Thorne 1973)

$$S^i{}_{;i} = \frac{1}{T}\left[2\eta\sigma^2 - q^i\left(\frac{T_{,i}}{T} + a_i\right)\right], \tag{32}$$

where a^i is the 4-acceleration, σ^{ij} is the shear tensor, and $\sigma^2 = \sigma^{ij}\sigma_{ij}$. By considering the total stress-energy tensor $T^{ij} = T^{ij}_M + T^{ij}_R$, we can assimilate radiative terms to dissipative contributions (see Appendix):

$$q^i = \mathcal{M}^i = w_1 e^i_{\hat{r}}\,,$$
$$2\eta\sigma^{ij} = \mathcal{M}^{ij} = \left(\frac{3}{2}\right)^{1/2}\frac{w_2}{\sigma}\,\sigma^{ij}\,. \tag{33}$$

The entropy generation is then obtained by integrating equations (32) over the 4-volume bounded by the two hypersurfaces τ and $\tau + d\tau$, where now τ is the proper time of the comoving observer. Apart from a dimensional constant, the entropy production rate is then

$$\dot{S} = -\int_0^\infty \frac{L}{T}\left\{vf\left[\frac{(yv)'}{yv} - 1\right] + \frac{(yT)'}{yT}\right\} d\ln r\,, \tag{34}$$

where f is defined in equation (5). $\dot{S}$ was evaluated for each HL and LL model; for the same $\dot{m}$ the former always show a much larger entropy production rate, and this can be regarded as a hint of the instability of HL solutions. We are aware that this analysis gives by no means a definite proof, and an investigation of the full time-dependent problem is needed.

5. CONCLUSIONS

In this paper we have presented a self-consistent model for stationary, spherical accretion onto a Schwarzschild black hole. By making use of a fully general relativistic approach and solving the complete transfer problem under no simplifying assumption, we were able to compute solutions in a wide range of accretion rates, ranging from optically thin to optically thick regimes. We discussed carefully the presence of critical points in the coupled system of equations describing radiation hydrodynamics and their role in freezing free conditions; in particular we stressed the existence of a second critical point, besides the hydrodynamical one, connected with the radiation field. Several models were computed in a range of $\dot{m}$ spanning more than four decades. Results were then used to construct a complete and consistent (log $\dot{m}$, log l)-diagram which, confirming previous analysis, shows that two distinct branches of solutions with very different emission properties are present. The nonexistence of high-luminosity models outside a defined range of $\dot{m}$, $2 \lesssim \dot{m} \lesssim 100$, is explained as the result of Compton heating of the gas near or interior to the sonic radius, by evaluating both "classical" and "generalized" preheating limits in a consistent way with the actual value of the radiation temperature. We briefly addressed also the issue of stability of solutions, giving some hints about the instability of HL models.

Finally we point out that some important aspects concerning stationary, spherical accretion are still open to further investigations, even leaving aside fundamental problems like the presence of magnetic fields and dissipation, which require an approach rather different from that presented here. Although we discussed in a semiquantitative way the properties of the emitted spectrum, a precise answer to this important question can be given only by solving the full, nongray transfer; such an approach is also needed for an exact determination of the radiation temperature and to take into account photoionization. A careful time-dependent analysis, incorporating all the physical inputs of the present stationary model, should be also undertaken to assess the stability of the two possible accretion modes. Both of these issues are presently under investigation.

APPENDIX

In this Appendix we derive hydrodynamical equations in the form of equation (11), starting from the conservation laws $T^{ij}{}_{;j} = 0$. The general expression for the radiation stress-energy tensor can be written in terms of the first three PSTF moments as

$$T^{ij}_R = \tfrac{4}{3}\mathcal{M}u^i u^j + \tfrac{1}{3}\mathcal{M}g^{ij} + 2\mathcal{M}^{(i}u^{j)} + \mathcal{M}^{ij} \tag{A1}$$

where u^i is the flow 4-velocity and g^{ij} is the metric tensor. In the particular case of spherical symmetry the PSTF moments take the simple form

$$\mathcal{M} = w_0\,, \qquad \mathcal{M}^i = w_1 e^i_{\hat{r}}\,, \qquad \mathcal{M}^{ij} = w_2(e^i_{\hat{r}}\,e^j_{\hat{r}} - \tfrac{1}{2}e^i_{\hat{\theta}}\,e^j_{\hat{\theta}} - \tfrac{1}{2}e^i_{\hat{\phi}}\,e^j_{\hat{\phi}})\,, \tag{A2}$$

where

$$e^i_{\hat{0}} = u^i\,, \qquad e^i_{\hat{r}} = a^i/a\,, \qquad e^i_{\hat{\theta}} = (0, 0, r^{-1}, 0)\,, \qquad e^i_{\hat{\phi}} = (0, 0, 0, (r \sin\theta)^{-1}) \tag{A3}$$

is the tetrad carried by the comoving observer (Thorne 1981; Thorne et al. 1981). By introducing the fluid spatial velocity v as measured by a stationary observer and $y = [(1 - 1/r)/(1 - v^2)]^{1/2}$, the 4-velocity and the 4-acceleration become

$$u^i = \left(\frac{y}{-g_{00}}, vy, 0, 0\right), \qquad a^i = \frac{dy}{dr}\left(\frac{vy}{-g_{00}}, y, 0, 0\right), \tag{A4}$$

$a = dy/dr$. The total stress-energy tensor for the gas plus radiation medium is given by $T^{ij} = T^{ij}_M + T^{ij}_R$, and

$$T^{ij}_M = (P + \rho)u^i u^j + \tfrac{1}{3}Pg^{ij}\,, \tag{A5}$$

if matter can be treated as a perfect fluid. The hydrodynamical equations are then obtained by taking the 4-divergence of T^{ij} and projecting it along $e^i_{\hat{0}}$ and $e^i_{\hat{r}}$, to obtain the local energy and r-momentum component conservation, respectively. After some algebra, by making use of the baryon conservation law

$$(\rho_0 u^i)_{;i} = (\rho_0)_{;i} u^i + \rho_0 \Theta = 0 \tag{A6}$$

and recalling that

$$\Theta = u^i_{;i} = \frac{1}{r^2}\frac{d}{dr}(r^2 vy)\,,$$

the equations can be written as

$$\begin{aligned}
&(P + \rho)\frac{dy}{dr} + y\frac{dP}{dr} + \frac{4}{3}w_0\frac{dy}{dr} + \frac{1}{3}y\frac{dw_0}{dr} + \frac{1}{yvr^2}\frac{d}{dr}(y^2v^2r^2w_1) + \frac{1}{r^3}\frac{d}{dr}(r^3yw_2) = 0\,,\\
&\frac{d\rho}{dr} - \frac{P + \rho}{\rho_0}\frac{d\rho_0}{dr} + \frac{dw_0}{dr} + \frac{4}{3}\frac{w_0}{yvr^2}\frac{d}{dr}(yvr^2) + \frac{1}{y^2vr^2}\frac{d}{dr}(y^2r^2w_1) + w_2\frac{r}{yv}\frac{d}{dr}\left(\frac{yv}{r}\right) = 0\,.
\end{aligned} \tag{A7}$$

The final step consists in eliminating the radiation terms in equations (A7) via the radiative transfer equations (4), written as

$$\begin{aligned}
&\frac{1}{y^2vr^2}\frac{d}{dr}(y^2r^2w_1) + \frac{4}{3}\frac{w_0}{yvr^2}\frac{d}{dr}(yvr^2) + \frac{dw_0}{dr} + w_2\frac{r}{yv}\frac{d}{dr}\left(\frac{yv}{r}\right) = \frac{s_0}{yv}\,,\\
&\frac{1}{yvr^2}\frac{d}{dr}(y^2v^2r^2w_1) + \frac{1}{3}y\frac{dw_0}{dr} + \frac{4}{3}w_0\frac{dy}{dr} + \frac{1}{r^3}\frac{d}{dr}(r^3yw_2) = s_1\,.
\end{aligned} \tag{A8}$$

Upon this substitution, equations (A7) yield precisely equations (11).

REFERENCES

Begelman, M. C. 1978, A&A, 70, 583
———. 1979, MNRAS, 187, 237
Bisnovatyi-Kogan, G. S., & Blinnikov, S. I. 1980, MNRAS, 191, 711
Blandford, R. D., & Payne, D. G. 1981, MNRAS, 194, 1033
Blondin, J. M. 1986, ApJ, 308, 755
Bondi, H. 1952, MNRAS, 112, 195
Buff, J., & McCray, R. 1974, ApJ, 189, 147
Chandrasekhar, S. 1960, Radiative Transfer (New York: Dover)
Chang, K. M., & Ostriker, J. P. 1985, ApJ, 288, 428
Colpi, M. 1988, ApJ, 326, 223
Cowie, L. L., Ostriker, J. P., & Stark, A. A. 1978, ApJ, 226, 1041
Essex, C. 1984, ApJ, 285, 279
Flammang, R. A. 1982, MNRAS, 199, 833
———. 1984, MNRAS, 206, 589
Freihoffer, D. 1981, A&A, 100, 178
Gilden, D. L., & Wheeler, J. C. 1980, ApJ, 239, 705
Gillman, A. W., & Stellingwerf, R. F. 1980, ApJ, 240, 235
Kafka, P., & Mészáros, P. 1976, Gen. Rel. Grav., 7, 841
Mészáros, P. 1975, A&A, 44, 59
Michel, F. C. 1972, Ap&SS, 15, 153
Moncrief, V. 1980, ApJ, 235, 1083
Nobili, L., Calvani, M., & Turolla, R. 1985, MNRAS, 214, 161
Nobili, L., & Turolla, R. 1988, ApJ, 333, 248
Novikov, I. D., & Thorne, K. S. 1973, in Black Holes, ed. C. De Witt & B. S. DeWitt (New York: Gordon & Breach), 343
Ostriker, J. P., McCray, R., Weaver, R., & Yahil, A. 1976, ApJ, 208, L61
Park, M.-G. 1990a, ApJ, 354, 64
———. 1990b, ApJ, 354, 83
Park, M.-G., & Ostriker, J. P. 1989, ApJ, 347, 679
Payne, D. G., & Blandford, R. D. 1981, MNRAS, 196, 781
Rybicki, G. B., & Lightman, A. P. 1979, Radiative Processes in Astrophysics (New York: Wiley)
Schmid-Burgk, J. 1978, Ap&SS, 56, 191
Service, A. T. 1986, ApJ, 307, 60
Shapiro, S. L. 1973a, ApJ, 180, 531
———. 1973b, ApJ, 185, 69
Shull, J. M. 1979, ApJ, 229, 1092
Shvartsman, V. F. 1971, Soviet Astr.—AJ, 15, 377
Soffel, M. H. 1982, A&A, 116, 111
Stellingwerf, R. F., & Buff, J. 1978, ApJ, 221, 661
———. 1982, ApJ, 260, 755
Tamazawa, S., Toyama, K., Kaneko, N., & Ôno, Y. 1974, Ap&SS, 32, 403
Thorne, K. S. 1981, MNRAS, 194, 439
Thorne, K. S., Flammang, R. A., & Żytkow, A. N. 1981, MNRAS, 194, 475
Turolla, R., & Nobili, L. 1988, MNRAS, 235, 1273
———. 1989, ApJ, 342, 982
Vitello, P. A. J. 1978, 225, 694
———. 1984, ApJ, 284, 394
Wandel, A., Yahil, A., & Milgrom, M. 1984, ApJ, 282, 53